Water Practice & Technology

IWA PUBLISHING

Water Practice & Technology Vol 18 No 5, 1022 doi: 10.2166/wpt.2023.054

Efficient adsorption of nickel and chromium(VI) from aqueous solutions using lignocellulose nanofibers: Kinetics, isotherms, and thermodynamic studies

Meghdad Sheikhi[a,*] and Hassan Rezaei[b]

[a] Environmental Pollution, Islamic Azad University Science and Research Branch Tehran, Tehran, Iran
[b] Environmental Science Department, Gorgan University of Agricultural Sciences and Natural Resources, Gorgan, Iran
*Corresponding author. E-mail: meghdad_sheikhi@yahoo.com

ABSTRACT

The entry of heavy metals due to industrial activities into the environment is one of the major problems in this century. Nickel and chromium(VI) are the toxin elements that are used in various industries. In this study, lignocellulose nanofiber was purchased from the Nano-Novin Polymer Company (Gorgan, Iran) and used as an adsorbent for the removal of nickel and chromium(VI) ions from aqueous solutions in a batch system. The effects of pH, initial concentration, adsorbent dose, contact time, and temperature were investigated. The adsorption mechanism was determined by Langmuir, Freundlich, kinetic, and thermodynamic models. Investigation of equilibrium isotherms nickel and chromium(VI) showed that the isotherm fitted well with the Freundlich model. The pseudo-second-order model with the larger correlation coefficient had a greater fitness against experimental data in the kinetic studies. Thermodynamic parameters of both nickel and chromium such as Gibbs free energy, enthalpy, and entropy were calculated which indicated spontaneous, endothermic, and random processes, respectively. Lignocellulose nanofiber can be suggested as a good adsorbent that is highly capable of adsorbing nickel and chromium(VI) from aqueous solutions.

Key words: adsorption, chromium(VI), isotherm, lignocellulose nanofiber, nickel

HIGHLIGHTS

- Lignocellulose nanofiber was purchased from the Nano-Novin Polymer Company.
- Lignocellulose nanofiber as a good adsorbent is highly capable of adsorbing nickel and chromium from aqueous solutions.
- The effects of pH, initial concentration, adsorbent dose, contact time, and temperature were investigated.
- The adsorption mechanism was determined by Langmuir, Freundlich, kinetic, and thermodynamic models.

1. INTRODUCTION

Nowadays, with increasing environmental problems and concerns, caused by heavy metal pollution, various industries such as metallurgical plants, plating, alloys, and battery production, technologies to treat polluted water should be developed rapidly (Rodiguez *et al.* 2018). One of the most important environmental concerns is the pollution caused by the toxicity of heavy metal ions, which accumulates in the food chain and has a high shelf life in nature (Xavier *et al.* 2018). The use of heavy metals in various industries is increasing which leads to environmental pollution (Maleki *et al.* 2019) Heavy metal ions are found naturally in volcanic activity, and weathering of rocks, as well as in many industries. The discharge of metal-polluted wastewater (e.g., brine) degrades water quality and thus water cannot be directly used for potable water (via desalination) and industrial applications (Panagopoulos 2022a, 2022b; Panagopoulos & Giannika 2022).

There are various methods for the purification of heavy metal ions in an aqueous solution, including chemical deposition, ion exchange, membrane filtration, precipitation, electrolytic method, reverse osmosis, solvent extraction, and adsorption (Manjuladevi *et al.* 2018; Anand *et al.* 2019; Kumar *et al.* 2019a, 2019b). Among all these methods, the adsorption method is preferred to other methods due to proper filtration, easy efficiency, and availability of various adsorbents (Zhang *et al.* 2018). The type of adsorbent and its method is essential in the adsorption method. In recent decades, the study of adsorbents has been expanded because they are highly effective, cheap, and economical (Kong *et al.* 2018).

The wide spread of nickel as a toxic heavy metal in the environment is harmful to human health. Ni(II) pollution in the aquatic environment is mainly caused by mines, melting, coal combustion, and plating (Yu *et al.* 2019). Once nickel enters the body, it penetrates all organs and accumulates in various tissues, causing damage to them, which may cause nerve, liver, kidney, and reproductive damage, and increase the risk of cancer (Shi *et al.* 2018). The high amount of nickel in the human body is dangerous to the skin (Zhou *et al.* 2018). Chromium is a natural element that is found mostly in nature in the form of trivalent and hexavalent chromium. Hexavalent chromium is more toxic than trivalent chromium (Arim *et al.* 2018). Chromium enters the human body through the skin, inhalation, or oral consumption and is transmitted by blood to the kidneys and liver. Hexavalent chromium is carcinogenic and damages DNA (Shi *et al.* 2018). Due to the high solubility of chromium in water, its accumulation is common in aqueous environments (Rizzo *et al.* 2019). Hexavalent chromium(VI) is a highly toxic heavy metal that is used in various industries such as leather, catalysts, fungicides, pigment production, ceramics, art, glass, photography, plating, etc. (Peng *et al.* 2019). Chromium causes problems such as bronchitis, cancer, wound formation, liver damage, weakened immune system, respiratory problems, and kidney damage (Gebru & Das 2018). The chromium(VI) concentration in drinking water used for human consumption may not be higher than 0.05 mg L^{-1}, and the maximum allowable concentration in water and wastewater for the final discharge in the environment is 0.1 mg L^{-1} (Vilela *et al.* 2019).

Many inexpensive biopolymers such as chitosan, chitin, pectin, starch, cellulose, bacterial cellulose, lignin, and hemicellulose have been grafted with a variety of vinyl monomers for their use in separation technologies (Kumar & Sharma 2019) Cellulose is one of the most natural and plentiful renewable polymers (Kumar *et al.* 2019a, 2019b). Lingo cellulose is an ideal biological adsorbent because it is renewable, cheap, and has special structural properties. The main components of lignocelluloses are cellulose, hemicellulose, and lignin and it includes different kinds of functional groups such as hydroxyl, acetyl, phenolic, carboxyl, and methyl (An *et al.* 2018).

Removal of heavy metals through the application of various adsorbents has been of interest to many researchers because removal of this substance from wastewater before discharge into aquatic systems is necessary. Various technologies have been used in the past including chemical deposition, adsorption, ion exchange, membrane separation, solvent extraction, and biological processes to remove heavy metals from water and wastewater. Among these technologies, adsorption is the most appropriate method due to its high efficiency, low cost, convenient preparation, and operation. In the current study, the adsorption process was used to remove nickel and chromium(VI) ions. Adsorption is favored over other techniques due to ease of operation, low energy input, and removal of pollutants even at trace concentrations. The removal of nickel and chromium(VI) ions can be achieved by using various adsorbents like pomelo peel (Wu *et al.* 2017), Nano Kaolinite (Alasadi *et al.* 2019), Eichhornia crassipes and Lemna minor (Balasubramanian *et al.* 2019), microwave-functionalized cellulose (Qu *et al.* 2020), and coconut shell (Bal and Bhasarkar).

In this study, the application of lignocellulose nanofiber was investigated for the adsorption of nickel and hexavalent chromium from aqueous solutions in a batch system. The main objectives of this study were to investigate the effect of pH, initial concentration, contact time, temperature, and adsorbent dose on the adsorption of nickel and hexavalent chromium from aqueous solutions using lignocellulose nanofiber. For determining the mechanism of the adsorption in this study kinetic, thermodynamic, and adsorption isotherm models were investigated.

2. BACKGROUND

2.1. Lignocellulose nanofiber

Cellulose as a natural and renewable material has valuable physical properties which can be improved with detailed knowledge of the structure (Peter 2020). In addition, cellulose is the most abundant biomaterial and natural regenerating polymer (Ji *et al.* 2020). Lignocellulose nanofiber is composed of cellulose, hemicellulose, and lignin, and its raw materials include wood and other lignocellulose residues (e.g., wheat straw, rice straw, and sugarcane bagasse). This study used lignocellulose nanofiber for the adsorption of nickel and chromium(VI) ions from aqueous solutions. The advantages of this adsorbent over other adsorbents are specific surface area and ease of separation from the soluble phase (Zhang *et al.* 2020).

Cellulose nanofiber is typically produced using various mechanical methods such as homogenization, microfluidization, micro-grinding, refining, cryocrushing, or in combination with chemical and enzymatic pretreatments (Ferrer *et al.* 2012; Brodin *et al.* 2014). Many studies have been carried out on the use of cellulose nanofiber produced from virgin fiber as a strengthening agent for improving the physical and mechanical

properties of paper, while the use of cellulose nanofiber isolated from bleached virgin fiber is not necessary or reasonable for many recycled/impure products (Yousefhashemi *et al.* 2019).

Lignocellulose nanofiber has been produced from cheap, recycled, old, corrugated container pulp by the use of an ultra-fine grinding technique. The diameter of the lignocellulose nanofiber is in the range of 10–80 nm, and the cellulose crystallinity index and crystallite size is 49% and 4 nm, respectively, during the process (Yousefhashemi *et al.* 2019).

3. MATERIALS AND METHODS

3.1. Materials

This study was conducted on lignocellulose nanofiber as an adsorbent of heavy metal chromium(VI) and nickel ions from aqueous solutions on a laboratory scale in the Science and Research Branch of Azad University, Tehran, with two batch replications. Lignocellulose nanofiber was purchased from the Nano-Novin Polymer Company (Gorgan, Iran) with the physiochemical properties of lignocellulose nanofiber as shown in Table 1. The other chemicals were purchased from Merck Company (Germany).

Table 1 | Properties of the Nano-Novin Polymer

Name	Lignocellulose nanofibers gel
Compounds	Lignin, cellulose, hemicellulose
Material state	Gel
Color	Brown
Production method	Chemi-mechanical synthesis
Nanofiber diameter	Ave.: 55 nm

3.2. Adsorption experiments

Batch adsorption studies were carried out to evaluate the efficiency of lignocellulose nanofiber adsorbent on the removal of nickel and chromium(VI) from the aqueous solutions. The stock solution of 1,000 mg L^{-1} was prepared by adding a certain amount of $K_2Cr_2O_7$ and deionized water. The pH of each solution was adjusted using 0.1 M NaOH and 0.1 M HCl. Adsorption experiments were performed in the batch system. The pH of the solutions was measured using Crison pH Meter Basic 20. For agitation of the adsorbent and the heavy metal ions, the Heimolph Unimax 2010 shaker was used. For all treatments, the agitation speed was constant and equal to 120 rpm. After the reaction time, the lignocellulose nanofiber adsorbent was separated using a Kokusan H-108 centrifuge at 10 min and 4,000 rpm. Chromium(VI) and nickel ions concentration were measured using the Atomic Adsorption Device (AAS) model (Unicam-919). The effects of pH, adsorbent dose, contact time, initial concentration, and temperature were examined on the efficiency and adsorption capacity of nickel and chromium(VI) ions by the adsorbents. SPSS and Excel software were used for data analysis.

3.3. Analysis description and procedure

The experimental results were collected to identify the efficiency of adsorption criteria such as adsorption percentage, adsorption capacity, and breakthrough points at different operating conditions.

The adsorption percentage and adsorption capacity of the heavy metal chromium equilibrium were calculated using the following equations (Dehghani *et al.* 2017; Aslani *et al.* 2018):

$$A(\%) = \frac{C_0 - C_e}{C_0} \times 100 \quad (1)$$

$$q_e = \frac{(C_0 - C_e)V}{m} \quad (2)$$

In this formula, A is the percentage of adsorption; q_e is the amount of adsorption capacity; C_0 is the initial concentration of a metal ion in solution in milli grams per liter; C_e is the equilibrium concentration of metal ion in solution in milligrams per liter; m is the adsorbent mass in gram; and V is the volume of solution in liter.

The Langmuir equation is expressed by the following equation (Langmuir 1918):

$$q_e = \frac{q_{max} \times C_e b}{1 + C_e b} \tag{3}$$

$$\frac{C_e}{q_e} = \frac{1}{q_{\max} b} + \frac{C_e}{q_{\max}} \tag{4}$$

In this equation, C_e (mg·L^{-1}) is the equilibrium concentration of the metal ion in solution, q_e is the equilibrium adsorption value (mg·g^{-1}), q_m is the maximum adsorption capacity, and b is the equilibrium constant of adsorption.

The Freundlich equation is expressed by the following equation (Veloso *et al.* 2020):

$$q_e = K_f (C_e)^{1/n} \tag{5}$$

$$\ln q_e = \ln K_f + \frac{1}{n} \ln\, C_e \tag{6}$$

In this respect, q_e is the amount absorbed in mg·g^{-1}, C_e is the equilibrium concentration of the adsorbed ions in mg·L^{-1}, and K_f is the Freundlich constant.

The study of biological adsorption at the temperature range produces thermodynamic constants such as the change of free energy of Gibbs ($\Delta G°$), enthalpy change ($\Delta H°$), and entropy change ($\Delta S°$).

The free energy of Gibbs is expressed by the following equation (Ates & Basak 2019):

$$\Delta G = -RT \ln\, K_C \tag{7}$$

T refers to temperature (Kelvin), R is the ideal gas constant equal to 8.314 J·mol^{-1}·K^{-1}, and K_C is the thermodynamic equilibrium constant obtained from the following formula:

$$K_C = \frac{C_a}{C_e} \tag{8}$$

C_a refers to mg of adsorbent, which absorbs per liter of solution, and C_e refers to soluble equilibrium concentration in milli grams per liter.

According to the laws of thermodynamics, the free energy of Gibbs at constant temperature depends on the enthalpy changes and the entropy changes expressed by Vant Hoff's Equation (9) (Kumar *et al.* 2018):

$$\ln K_C = \frac{-\Delta H^\circ}{R} \frac{1}{T} + \frac{\Delta S^\circ}{R} \tag{9}$$

where $\Delta H°$ and $\Delta S°$ are obtained from the slope and intercept of the origin of the $\ln K_C$ graph in terms of $1/T$, respectively.

Pseudo-first-order kinetic is expressed by the following equation (Bao *et al.* 2020):

$$\ln\, (q_e - q_t) = \ln q_e - k_1 t \tag{10}$$

q_t and q_e are the amount of metal ions absorbed at time t (min) and at equilibrium time and k_1 is the pseudo-first-order rate constant, respectively.

Pseudo-second-order kinetic is expressed by the following equation (Mahmoud *et al.* 2020):

$$\frac{t}{q_t} = \frac{1}{k_2 q_e^2} + \frac{t}{q_e} \tag{11}$$

4. RESULTS AND DISCUSSION

4.1. Characterizations and properties of lignocellulose nanofiber

Fourier transform infrared spectroscopy (FTIR) and X-ray diffraction (XRD) were used to characterize the functional groups of the adsorbents and scanning electronic microscopy (SEM) was employed to observe the morphologies. Figure 1(a), the FTIR analysis was used to determine the superficial groups of lignocellulose nanofiber. As shown in Figure 3, in the FTIR spectrum of lignocellulose nanofibers, the wide peak (the left side) in the region of 2,800–3,600 cm^{-1} (3,359.81 cm^{-1}) is related to the –OH (hydroxyl) and –NH functional groups in the FTIR spectrum by lignocellulose nanofibers. The peak in the region of 1,601.20 cm^{-1} is related to the functional

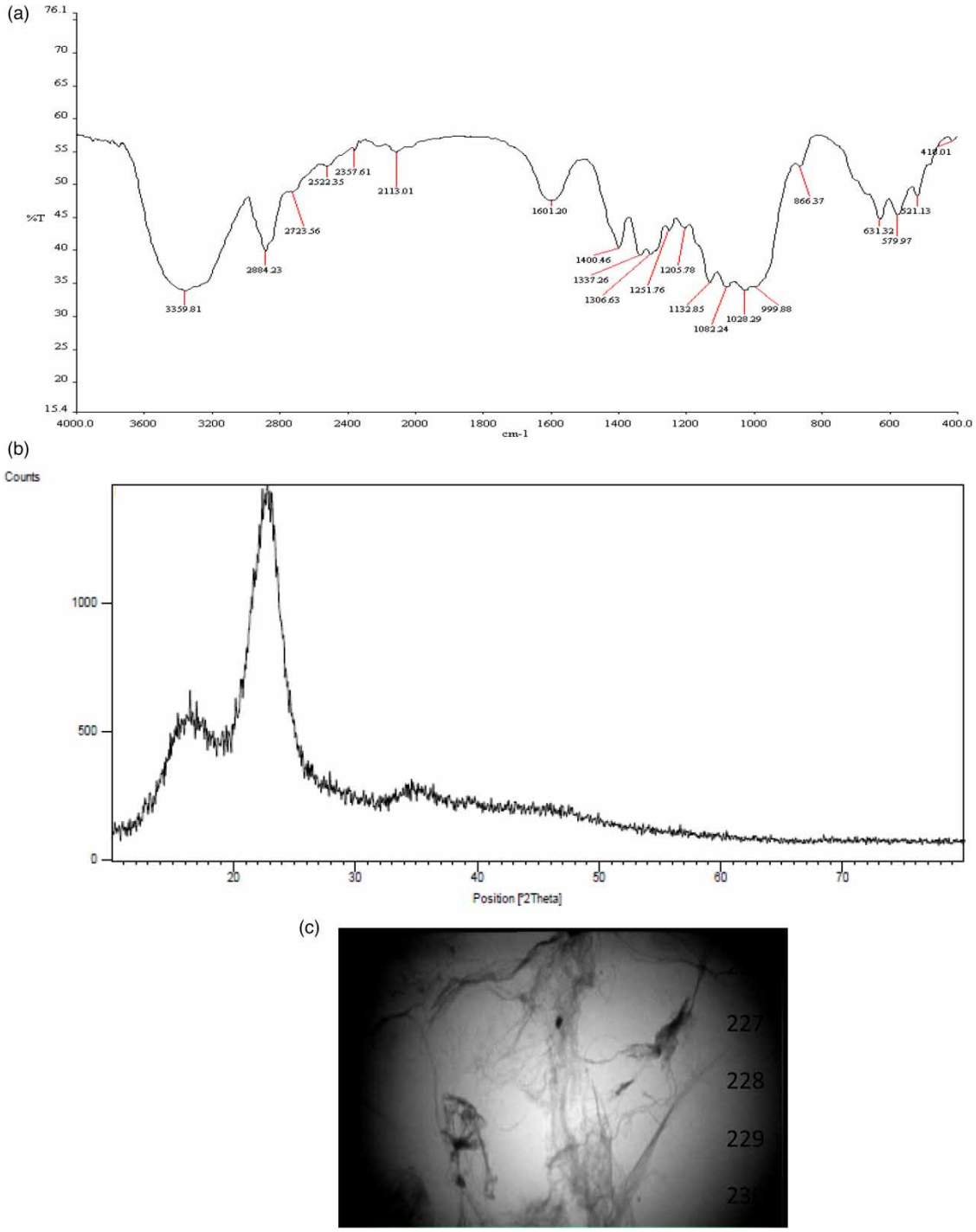

Figure 1 | FTIR analysis (a), X-ray diffraction (b), and TEM (c) of lignocellulose nanofibers.

group of C = O. The peak in the region of 1,028.29 cm^{-1} is related to the functional group of C–O. The next weak band in the region of 2,884.23 cm^{-1} after adsorption probably relates to the C–H functional groups. XRD analysis determines the crystalline structure of the adsorbent. As observed in Figure 1(b), the XRD curve of nano-crystalline peaks at 2θ is observed to be 16, 23, and 35.5, all indicating the crystalline structure of lignocellulose nanofiber. In order to study the diameter of lignocellulose nanofiber, transmission electron microscope (TEM) analysis was applied. According to Figure 1(c), the material used has less than 100 nm diameter (in the range of nanometers), and has a fibrous and network structure.

4.2. Effect of pH

The solution pH has a considerable effect on the uptake of metal ions because it indicates the surface charge of the adsorbent and the degree of ionization and speciation of the adsorbate (Balasubramanian *et al.* 2019). In the adsorption process, pH has an important role in the removal of heavy metals (Barsbay *et al.* 2018; Esmaeili & Beni 2018). Adsorption experiments were carried out in the pH range of 2–7, keeping all other parameters constant (initial concentration = 10 mg/L, adsorbent dose = 0.1 g, contact time = 60 min, and $T = 25$ °C). For all treatments, the agitation speed was constant and equal to 120 rpm**.** When the pH rises above 7, the nickel and chromium hydroxides become insoluble, the adsorption capacity of nickel and chromium decreases, so the pH above 7 has not been investigated (Guo *et al.* 2018). The results of nickel and chromium(VI) are given in Figure 2(a) and 2(b), respectively. When the pH increases, the adsorption efficiency of nickel and chromium increases, so the adsorption percentage of nickel and chromium adsorption at pH = 5 are 91.2 and 83.4, respectively. Then at pH 6 and 7, the adsorption efficiency and adsorption capacity decrease. The results showed that the adsorption of nickel and chromium is pH-dependent, which affects the adsorbent surface properties and adsorption efficiency. Other researchers reported similar results for the adsorption of nickel and chromium by different adsorbents (An *et al.* 2019; Dehghani *et al.* 2019; Sethy & Sahoo 2019).

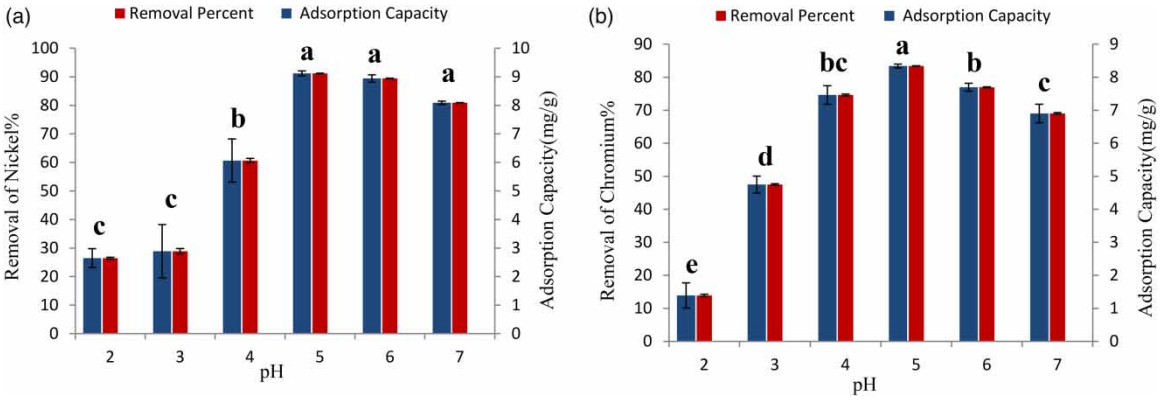

Figure 2 | The effect of pH on the adsorption percent-capacity of nickel and chromium(VI) ions by lignocellulose nanofibers (initial concentration = 10 mg/L, adsorbent dose = 0.1 g, contact time = 60 min, and $T = 25$ °C).

Statistical analysis of data by one-way ANOVA test indicated the directional effect of pH on the adsorption rate, which was significant ($p < 0.05$). Duncan's statistical test also showed that the optimum pH was 5. Duncan's test results also indicated significant differences in all cases, except the average pH of nickel at 5–7 and 2 and 3, the average pH of chromium at 4 and 6 and 4 and 7.

4.3. Effect of initial concentration of nickel and hexavalent chromium

The initial concentration is one of the important driving forces that affect the sorption process. The effect of changing the initial concentration of nickel and hexavalent chromium in the range of 5–50 mg/L while keeping the adsorbent dose (0.1 g), pH (6), contact time (60 min) and temperature (25 °C) constant are illustrated in Figure 5. For all treatments, the agitation speed was constant and equal to 120 rpm. According to Figure 3, the maximum adsorption percentages of nickel and chromium at concentration of 5 mg/L are 91.9 and 84.5%, respectively. However, at higher concentrations, the metal cations are far beyond the capacity of the receptors. As a result, competition for access to the contact area increases, and all connection sites are exposed to ions and are activated. The maximum adsorption capacity of nickel and chromium at concentration of 50 mg/L is 44.97 and

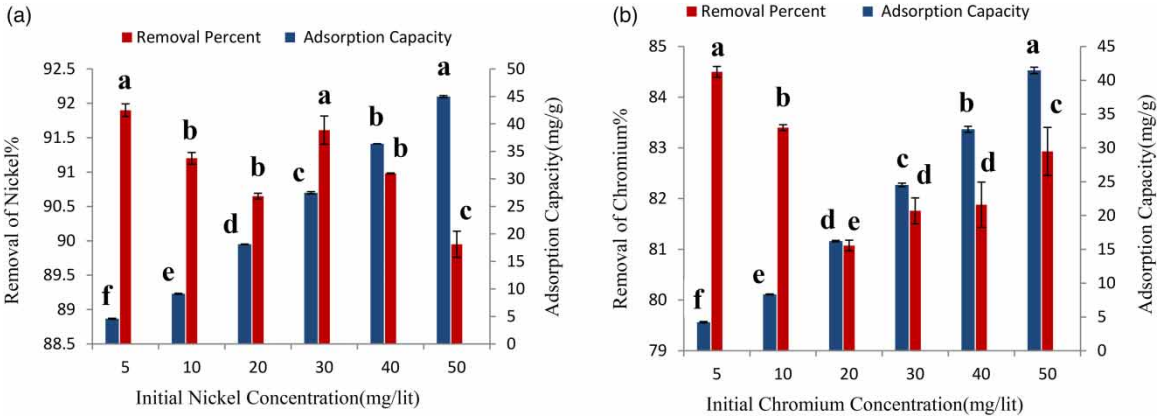

Figure 3 | The effect of concentration on the adsorption percent-capacity of nickel (a) and hexavalent chromium (b) ions by lignocellulose nanofibers (adsorbent dose = 0.1 g, pH = 5, contact time = 60 min, and $T = 25$ °C).

41.46, respectively. As the initial concentration increases, the adsorption capacity also increases (Aslan *et al.* 2018; Zhou *et al.* 2018). At low concentrations, nickel and chromium have more receptors to adsorb metal cations (Farokhi *et al.* 2018). As a result, nickel and chromium ions are simply able to bind to receptors on the surface, so the adsorption percentage increases. As can be seen in Figure 3, lignocellulose nanofibers have been investigated at different concentrations. The difference in the percentage of adsorption at the highest and lowest concentrations of nickel and chromium is small, which is 2 and 3% for nickel and chromium, respectively, which indicates good and satisfactory adsorption of adsorbent in different concentrations. Other researchers reported similar results for the adsorption of nickel and chromium by different adsorbents (Sivakumar *et al.* 2018; Mahmoud *et al.* 2020).

Statistical analysis of data by one-way ANOVA test indicated the directional effect of initial concentration on adsorption rate, which was significant ($p < 0.05$). Duncan test results of both nickel and chromium also indicated significant differences in all cases, except the average initial concentration of nickel at 5 and 30 and 10, 20, and 40 mg/g, and the average initial concentration of chromium at 30 and 40 mg/g.

4.4. Effect of adsorbent dose

The effect of adsorbent dose on nickel and chromium(VI) removal in the range of 0.1–0.6 g at fixed initial concentration nickel and chromium(VI) = 10 mg/L, pH = 5, contact time = 60 min, and $T = 25$ °C is shown in Figure 4. For all treatments, the agitation speed was constant and equal to 120 rpm. According to Figure 4, the maximum adsorption of nickel and chromium by lignocellulose nanofiber in the absorbent dose of 0.6 g is 96.65 and 92.7%, respectively. The adsorption capacity of the adsorbent dose is decreasing from 0.1 to 0.6 g,

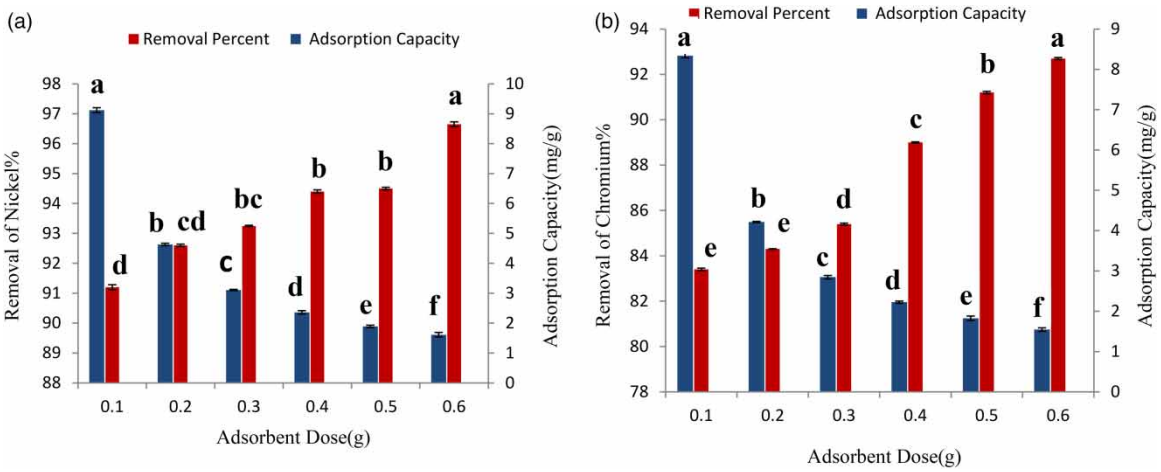

Figure 4 | The effect of adsorbent dosage on the adsorption percent-capacity of nickel (a) and hexavalent chromium (b) ions by lignocellulose nanofibers (initial concentration = 10 mg/L, pH = 5, contact time = 60 min, and $T = 25$ °C).

the maximum adsorption capacity of nickel and chromium in the adsorbent dose of 0.1 g is 9.12 and 8.34, respectively. The adsorption capacity declines with increasing adsorbent due to the increase in the number of unsaturated adsorption sites in the adsorbent (Sheikhi & Rezaei 2021). In general, the number of active adsorbent sites increases with the increase of adsorbent dose (Hadadian *et al.* 2018; Mousavi *et al.* 2019). As a result, the adsorption percentage increases. The maximum adsorption capacity of nickel and chromium at the adsorbent dose of 0.1 is 9.12 and 8.34, respectively, which indicates the high efficiency and cost-effectiveness of the adsorbent. As the adsorbent dose increases, the adsorption percentage of nickel and chromium ions increases because the number of adsorbable sites increases (Fan *et al.* 2019). Other researchers have found similar results for nickel and chromium uptake by different adsorbents (Hachoumi *et al.* 2019; Zhang *et al.* 2019).

Statistical analysis of data by one-way ANOVA test indicated the directional effect of adsorbent dose on adsorption rate, which was significant ($p < 0.05$). Duncan's statistical test also showed that the optimum adsorbent dose of nickel and chromium were 0.4 and 0.6 g, respectively. Duncan test results of both nickel and chromium also indicated significant differences in all cases, except the average adsorbent dose of nickel at 0.3, 0.4, and 0.5 and 0.2 and 0.3 g, and the average adsorbent dose of chromium at 0.1 and 0.2 g.

4.5. Effect of contact time

The effect of contact time was investigated within the range of 15–120 min, pH = 5, initial concentration of 5 mg·L^{-1} nickel and chromium, adsorbent dose of 0.1 g and temperature of 25 °C. As demonstrated in Figure 5, the adsorption increased with the test time. For all treatments, the agitation speed was constant and equal to 120 rpm**.** The highest adsorption rate of both nickel and chromium(VI) given as 96.4% was reached at 120 min. Figure 5 shows the effect of contact time on the adsorption percentage and adsorption capacity of nickel and chromium by lignocellulose nanofiber. As seen in Figure 5, the absorption rate increased from 15 to 120 min. Contact time must play an important role in the adsorption of heavy metals (Huang *et al.* 2018). Each substance must have a specific contact time to complete the adsorption process. Therefore, the adsorption property is highly dependent on the mixing time between the adsorbed substance and the adsorbent (Jiang *et al.* 2019). From the time of contact, it can be concluded that the amount of adsorption first increased and then reached equilibrium. Because of a larger number of active sites, the structure and area of the adsorbent are faster in the early times and allow the heavy metal to penetrate to a large extent (Bhowmik *et al.* 2018; Dim *et al.* 2021). Other researchers reported similar results for the adsorption of nickel and chromium by different adsorbents (Dim *et al.* 2021; Siuki *et al.* 2021).

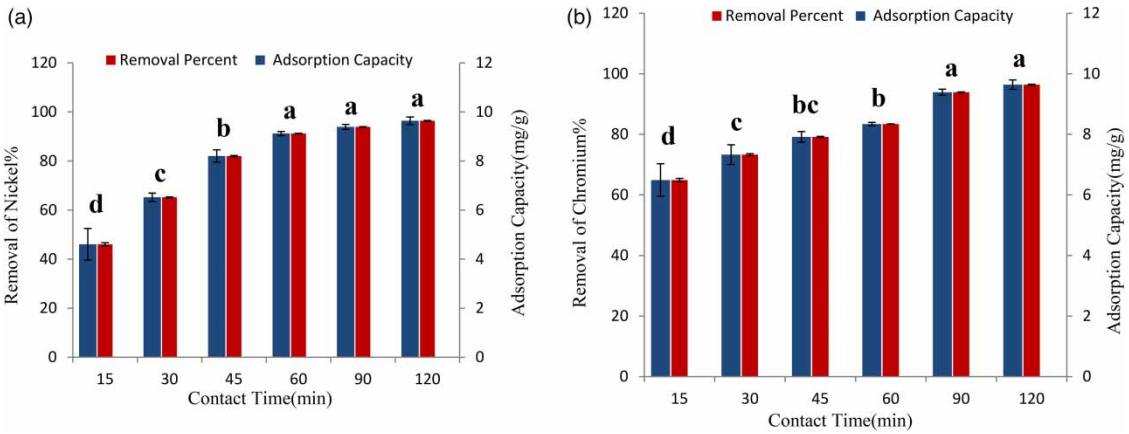

Figure 5 | The effect of contact time on the adsorption percent-capacity of nickel (a) and hexavalent chromium (b) ions by lignocellulose nanofibers (initial concentration = 10 mg/L, pH = 5, adsorbent dose = 0.1 g, and $T = 25$ °C).

In addition, statistical analysis of data by one-way ANOVA test indicated the directional effect of contact time on adsorption rate, which was significant ($p < 0.05$). Duncan's statistical test also showed that the optimum contact time of nickel and chromium were 60 and 90 min, respectively. Duncan test results of both nickel and chromium also indicated significant differences in all cases, except the average contact time of nickel at 60, 90, and 120 min, and the average contact time of chromium at 30 and 45 and 45 and 60 min.

4.6. Effect of temperature

Temperature plays a significant role in the chemical reaction between nickel and chromium(VI) with lignocellulose nanofiber. The adsorption experiments were conducted in the temperature range of 15–40 at constant nickel and chromium(VI) initial concentration (5 mg/L), pH (6), adsorbent dose (0.1 g/L) and contact time (60 min). For all treatments, the agitation speed was constant and equal to 120 rpm**.** The proper temperature can enhance the ion exchange and collision of atoms thereby improving the adsorption process (Shao *et al.* 2019). As can be seen in Figure 6, nickel adsorption by lignocellulose nanofiber increased from 54.75 to 97.15% with increasing temperature from 15 to 40 °C, and adsorption of Cr(VI) went up from 73.8 to 89.15% with the increase of temperature from 15 to 40 °C. According to Figure 6, adsorption went up with temperature because this adsorbent is not homogenous and the activation energies of adsorption sites vary. Therefore, at a low temperature, only the adsorption sites with low activation energy were occupied, while those with higher activation energy could be occupied only at higher temperatures (Kaewsichan & Tohdee 2019). The result obtained here is in agreement with the findings of other researchers who reported the adsorption of nickel and chromium by different adsorbents (Kundu *et al.* 2019; Mousavi *et al.* 2019).

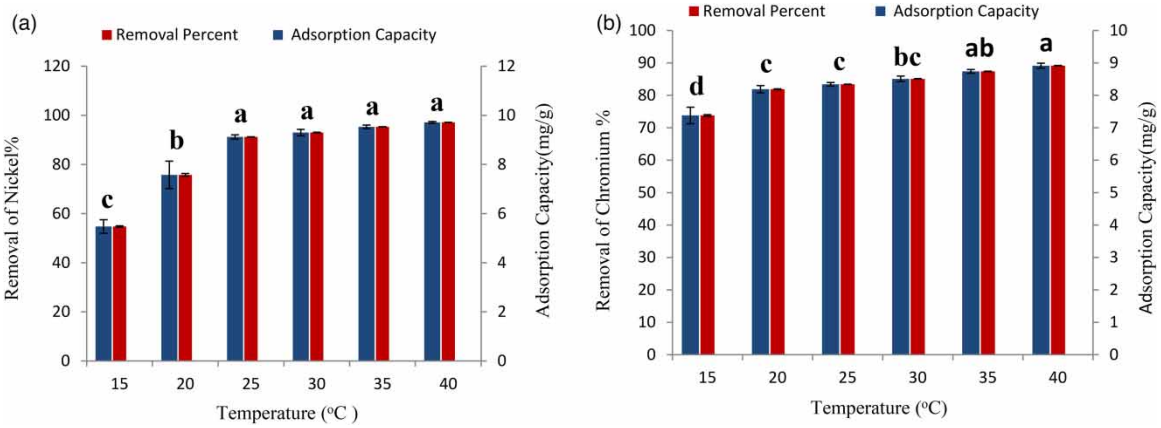

Figure 6 | The effect of temperature on the adsorption percent-capacity of nickel (a) and hexavalent chromium (b) ions by lignocellulose nanofibers (initial concentration = 10 mg/L, pH = 5, contact time = 60 min, and adsorbent dose = 0.1 g).

Statistical analysis of data by one-way ANOVA test indicated the directional effect of temperature on the adsorption rate, which was significant ($p < 0.05$). Duncan's statistical test also showed that the optimum temperature of nickel and chromium were 25 and 30 °C, respectively. Duncan test results of both nickel and chromium also indicated significant differences in all cases, except the average temperature of nickel at 25, 30, 35, and 40 °C, the average temperature of chromium at 20, 25, and 30, 30 and 35 °C, and 35 and 40 °C.

4.7. Adsorption isotherms

There are many models that can express the relationship between adsorption and residual concentration in solutions. Langmuir and Freundlich are more common and acceptable adsorption isotherms for the measurement of the adsorption of heavy metals in aqueous solutions (Hosseini *et al.* 2016). Therefore, in this study, Langmuir and Freundlich models have been applied to investigate and analyze experimental data and descriptions of the adsorption equilibrium between solid and liquid phases. The Langmuir model assumes uniform adsorption on the surface and is valid for monolayer adsorption with a homogeneous distribution of the adsorption sites and adsorption energies, while the Freundlich model shows multi-layer adsorption (Khelifi *et al.* 2018; Sun *et al.* 2019).

According to Figures 7 and 8 and Table 2 data, the Freundlich model with $R^2 = 0.9956$ (nickel) and $R^2 = 0.9951$ (chromium) compared to Langmuir with $R^2 = 0.5795$ (nickel) and $R^2 = 0.2379$ (chromium) can better describe the adsorption of nickel and chromium ions by lignocellulose nanofiber indicating that the data are consistent with the Freundlich model (Sohail *et al.* 2020). Maximum adsorption capacity (q_{max}) of nickel and chromium(VI) were equal to 270.271 and 344.827 mg·g^{-1}, respectively, which indicates that the adsorbent has

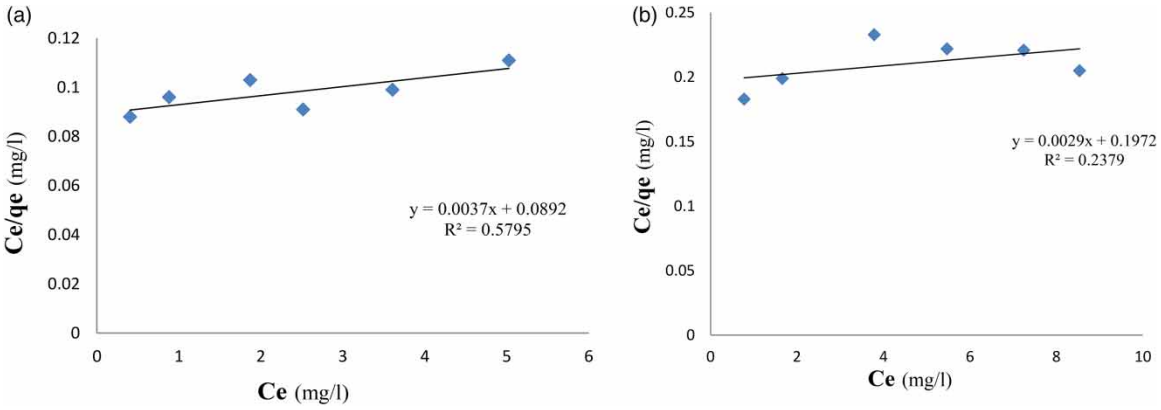

Figure 7 | Langmuir adsorption isotherm curve for nickel (a) and hexavalent chromium (b) ions absorption using lignocellulose nanofibers.

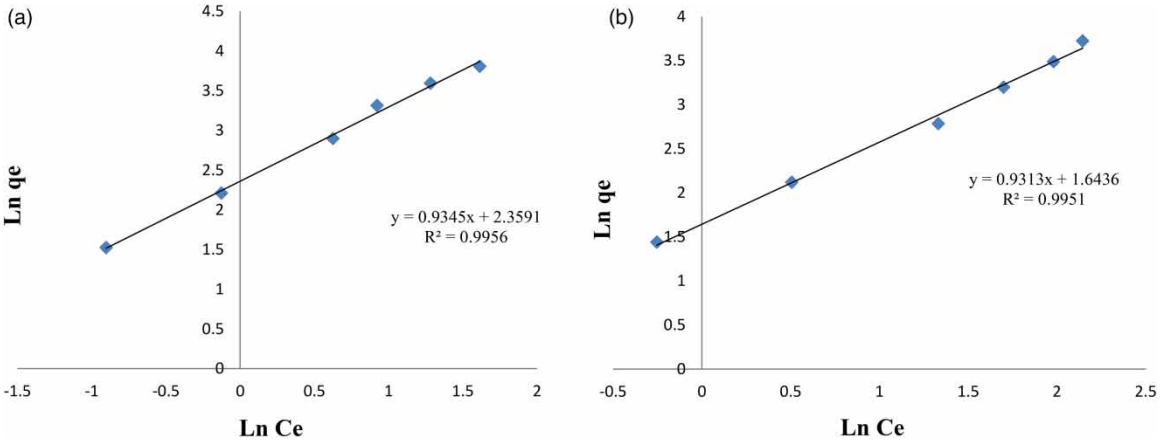

Figure 8 | Freundlich adsorption isotherm curve for nickel (a) and hexavalent chromium (b) ions absorption using lignocellulose nanofibers.

Table 2 | Langmuir and Freundlich constants and coefficients in the adsorption of nickel and chromium(VI) using lignocellulose nanofibers

Heavy metals	Freundlich isotherm model			Langmuir isotherm model		
Nickel	$K_f = 10.58$	$n = 1.07$	$R^2 = 0.9956$	$b = 0.041$	$q_{max} = 270.271$	$R^2 = 0.5795$
Chromium(VI)	$K_f = 5.17$	$n = 1.073$	$R^2 = 0.9951$	$b = 0.0147$	$q_{max} = 344.827$	$R^2 = 0.2379$

a relatively high adsorption capacity. Thus, the adsorbent can absorb heavy metals in high concentrations. The equilibrium constant of adsorption (b) of nickel and chromium(VI) was equal to 0.041 and 0.0147, respectively.

The calculated values of the Langmuir constant (K_L) show a proper affinity of adsorption sites for nickel and chromium ions with lignocellulose nanofiber. Based on the calculated value of separation factor R_L, its magnitude indicates the shape of the isotherm to be either favorable ($0 < R_L < 1$), unfavorable ($R_L > 1$), linear ($R_L = 1$), or irreversible ($R_L = 0$) (Al-Abbad *et al.* 2020).

As can be seen in Table 2, K_f is the Freundlich constant related to the bonding energy (L/g), and n is an empirical constant characterizing the heterogeneity of the process (g/L). According to the Freundlich model assumptions, if $n < 1$, the adsorption process is unfavorable, while if $1 < n > 10$, the adsorption process is favorable. Results show that n in nickel and chromium were equal to 1.07 and 1.073, respectively, which indicated the favorable process for this adsorbent. Table 2 shows the constant coefficients and correlation coefficients of the Langmuir and Freundlich isotherms in chromium adsorption using lignocellulose nanofiber.

Since R^2 is larger in Freundlich, the adsorption isotherm follows the Freundlich model. Freundlich isotherm is applicable to adsorption processes that occur on heterogonous surfaces. This isotherm gives an expression, which defines the surface heterogeneity and the exponential distribution of active sites and their energies.

4.8. Models of adsorption kinetics

The study of adsorption kinetics is essential to study the adsorption contact time (Mousavi *et al.* 2019). Adsorption kinetics is an important factor in the evaluation of adsorbents because it shows the amount of ions adsorbed by the adsorbent (Qureshi *et al.* 2017; Siddiqui *et al.* 2020). Adsorption kinetics models can be divided into two groups: reaction-based models and diffusion-based models. Reaction-based models include pseudo-first-order, pseudo-second-order, and Elovich models, and diffusion-based models include intraparticle diffusion, external-film diffusion, and internal-pore diffusion (Sarici-Ozdemir 2012). The models used in this study included reaction-based models of pseudo-first-order and pseudo-second-order.

The pseudo-first-order kinetic equation is based on adsorbent capacity and is used when adsorption occurs through the diffusion process inside a boundary layer (physical adsorption), while for the pseudo-second-order kinetic model, the model assumes that a metal ion is adsorbed to the available (two polar) sorption sites of the sorbent. The rate of pseudo-second-order sorption depends on the mass of the heavy metal ion on the sorbent surface and the number of heavy metal ions adsorbed at equilibrium (Aigbe & Osibote 2020).

Table 3 illustrates the pseudo-first-order kinetics and pseudo-second-order kinetics parameters in the adsorption of nickel and chromium using lignocellulose nanofiber. In order to evaluate the applicability of these kinetic models to fit the experimental data, K_1 and K_2 constants were determined experimentally from the slope and intercept of straight-line plots. As displayed in Figures 9 and 10, the results of the kinetic equation analysis showed that the adsorption data of nickel and chromium(VI) by lignocellulose nanofiber correspond to the pseudo-second-order model with $R^2 = 0.99$. Thus, the adsorption data follow the pseudo-second-order kinetic model (Kumar *et al.* 2019a, 2019b).

Table 3 | Pseudo-first-order kinetics and pseudo-second-order kinetics parameters in the adsorption of nickel and chromium(VI) using lignocellulose nanofibers

	Pseudo-second-order kinetics		Pseudo-first-order kinetics	
Nickel	$K = 0.038$	$R^2 = 0.7681$	$K = 0.0873$	$R^2 = 0.9941$
Chromium(VI)	$K = 0.0356$	$R^2 = 0.6383$	$K = 0.0944$	$R^2 = 0.9959$

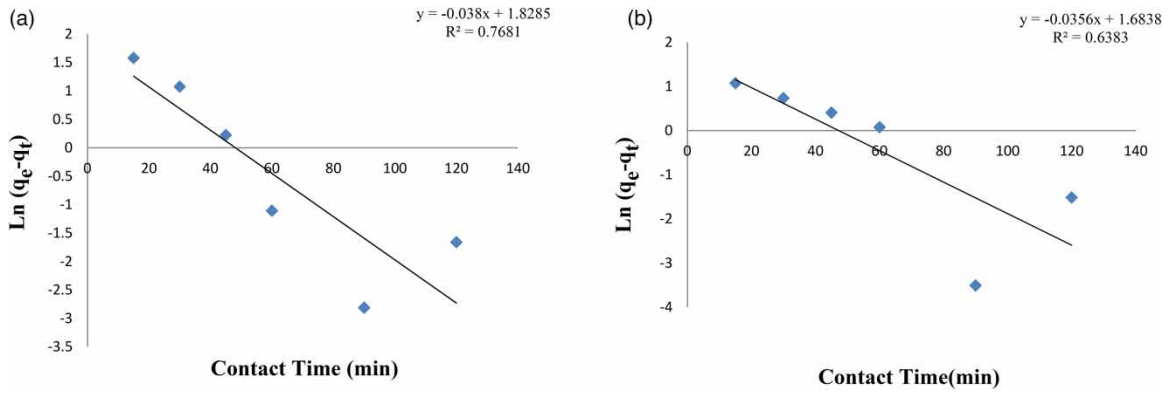

Figure 9 | Pseudo-first-order adsorption kinetics adsorption in nickel (a) and hexavalent chromium (b) ions absorption using lignocellulose nanofibers.

The analysis of the adsorption kinetics data according to the model Equations (10) and (11) resulted in the parameters listed in Table 3. The plot of $\ln(q_e - q_t)$ vs. t should yield a straight line if the experimental data conform to this pseudo-first-order kinetic model. The plot of t/q_t vs. t will give a straight line if the experimental

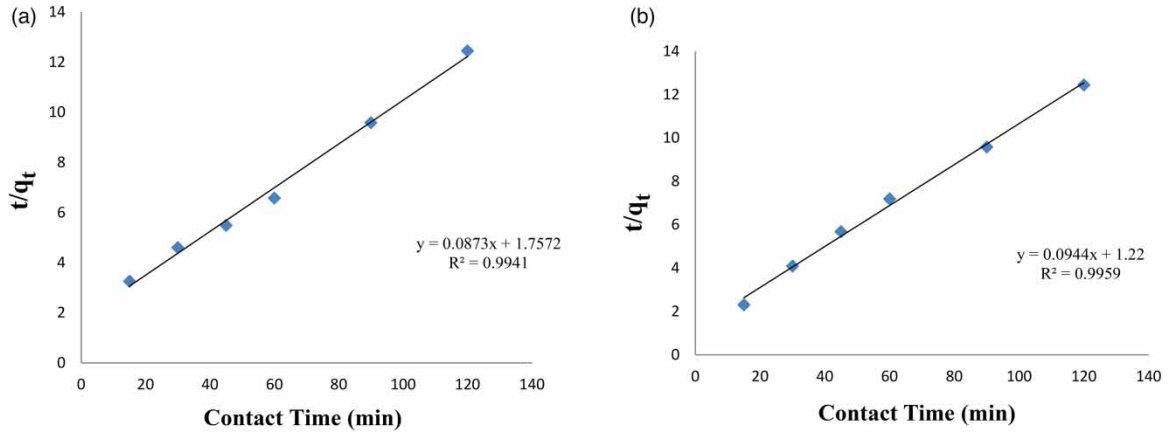

Figure 10 | Pseudo-second-order adsorption kinetics adsorption in nickel (a) and hexavalent chromium (b) ions absorption using lignocellulose nanofibers.

data conform to this pseudo-second-order kinetic model, and the values of q_e and K_2 are obtained, respectively, from the slope and intercept of such a plot.

The results indicated that both the pseudo-first-order equation kinetic model and the pseudo-second-order kinetic model were followed, but it fits more with the second-order equation. In this model, the rate-limiting step is the surface adsorption that involves chemisorption, where the removal from a solution is because of physicochemical interactions between the two phases. The model is usually represented by its linear form.

4.9. Thermodynamics

Thermodynamic parameters were obtained by varying temperature conditions over the range of 10–40 °C by keeping other variables constant. The values of the thermodynamic parameters such as $\Delta G°$, $\Delta H°$, and $\Delta S°$, describing nickel and chromium(VI) ions uptake by lignocellulose nanofibers, were calculated using the thermodynamic equations. The thermodynamic parameter indicates whether the adsorption reaction is spontaneous, random, exothermic, or endothermic.

Thermodynamic studies showed that the Gibbs free energy change ($\Delta G°$) indicates whether a chemical reaction would take place spontaneously, negative $\Delta G°$ confirms spontaneous adsorption, and positive $\Delta G°$ indicates its prohibition ($\Delta G° < 0$, $\Delta G° > 0$), $\Delta H°$ (enthalpy change) is the amount of energy released (exothermic process) or consumed (endothermic process) by adsorption ($\Delta H° < 0$, $\Delta H° > 0$). A positive $\Delta S°$ (change in entropy) specifies that the adsorption comprises a dissociative mechanism, while a negative $\Delta S°$ corresponds to an associative mechanism (Kaewsichan & Tohdee 2019).

As Figure 11 and Tables 4 and 5 illustrate, the process of nickel and chromium(VI) ions removal by lignocellulose nanofibers was demonstrated to be possible in terms of stoichiometry, indicating that the adsorption process is spontaneous. As the temperature rises, $\Delta G°$ is reduced; as a result, the spontaneous reaction of the

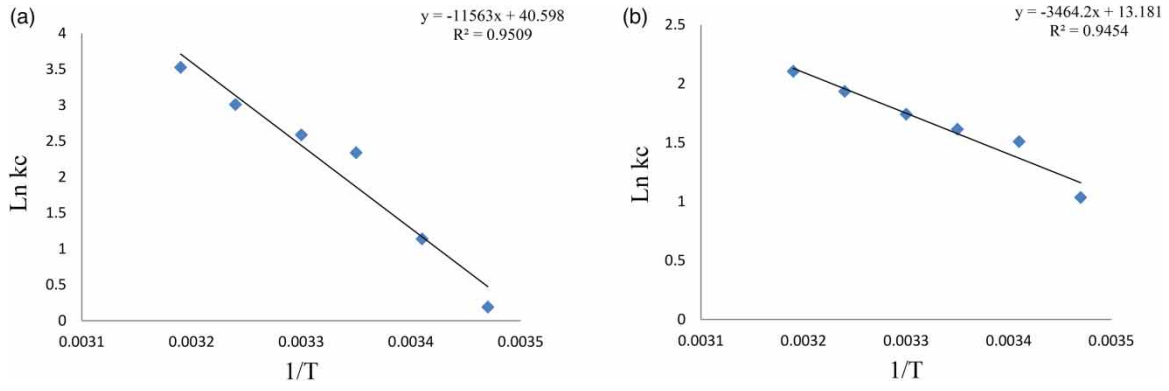

Figure 11 | Thermodynamics in nickel (a) and hexavalent chromium (b) ions absorption using lignocellulose nanofibers.

Table 4 | Thermodynamic parameters of nickel adsorption using lignocellulose nanofibers

T (°C)	$\Delta G°$ (kJ·mol^{-1})	$\Delta H°$ (kJ·mol)	ΔS (J·mol·k)
15	−454.942	96,134.782	+337.531
20	−2774.606		
25	−5792.563		
30	−6514.501		
35	−7705.182		
40	−9180.85		

Table 5 | Thermodynamic parameters of chromium(VI) adsorption using lignocellulose nanofibers

T (°C)	$\Delta G°$ (kJ·mol^{-1})	$\Delta H°$ (kJ·mol)	ΔS (J·mol·k)
15	−2478.237	28,801.358	+109.586
20	−3675.927		
25	−3998.801		
30	−4388.345		
35	−4957.538		
40	−5480.405		

process was increased. Furthermore, the positive values of $\Delta H°$ (enthalpy) showed that the overall reaction process was endothermic, that is, the removal rate was declined by increasing the ambient temperature. The positive values of $\Delta S°$ (entropy) also indicated that the amount of irregularity was increased at the solid–liquid interface during the adsorption process. In fact, the positive value of $\Delta S°$ represents the affinity of adsorbent to adsorbate in the solution and some structural changes in adsorbent and adsorbate.

The thermodynamics of nickel and chromium adsorption at various temperatures were studied according to Tables 4 and 5 where Gibbs free energy ($\Delta G°$), enthalpy ($\Delta H°$), and entropy ($\Delta S°$) were calculated.

As Tables 4 and 5 show, thermodynamic parameters of nickel and chromium(VI) adsorption using lignocellulose nanofiber $\Delta G°$, $\Delta H°$, and $\Delta S°$ are indicators of the possible nature of adsorption, spontaneous, endothermic, and random, respectively. Other researchers reported similar results for the adsorption of nickel and chromium by different adsorbents (Adebayo *et al.* 2020; Mondal & Chakraborty 2020).

5. CONCLUSION

In this study, the application of lignocellulose nanofiber was investigated for the adsorption of hexavalent chromium and nickel from aqueous solutions in a batch system. This study evaluated the effect of pH, temperature, contact time, initial Cr and Ni concentration, and adsorbent dose parameters on the percentage of adsorption and absorption capacity. The results showed that a pH of 6, an adsorbent dose of 0.1 g at 25 °C and 60 min of contact time offered the optimum percentages of adsorption in this research. The lignocellulose nanofiber proved to be excellent for the removal of nickel and chromium metal ions from aqueous solutions not only at low concentrations but at high concentrations too. The results of the study of two-parameter isotherms (Langmuir and Freundlich) revealed that in general, the studied isotherms well predicted the equilibrium of the system. The adsorption data fitted well the Freundlich isotherm model, showing that the adsorption of nickel and chromium on the adsorbent was multi-layered. Kinetic studies also showed that the data corresponded to the pseudo-second-order model and the intraparticle. The calculation of thermodynamic parameters of chromium and nickel showed a spontaneous, endothermic, and random process. Maximum adsorption capacity (q_{max}) of nickel and chromium(VI) was equal to 270.271 and 344.827 mg·g^{-1}, respectively, which indicates that the adsorbent has a relatively high adsorption capacity and cost-effectiveness of the adsorbent. Lignocellulose nanofiber, as the most abundant molecular biomass polymer in nature, has been characterized as possessing high biocompatibility, low toxicity, and high biodegradability properties. Thus, researchers are interested in such substances. According

to the results of this study, lignocellulose nanofiber has a high potential for the adsorption of chromium and nickel from aqueous solutions.

ACKNOWLEDGEMENTS

The authors thank The Islamic Azad University Science and Research Branch of Iran for providing laboratory materials and facilities. I would like to acknowledge the help and support of a dear friend, Arash Azizi, who provided me with certain resources while writing this paper.

DATA AVAILABILITY STATEMENT

All relevant data are included in the paper or its Supplementary Information.

CONFLICT OF INTEREST

The authors declare there is no conflict.

REFERENCES

Adebayo, G., Adegoke, H. & Fauzeeyat, S. 2020 Adsorption of Cr (VI) ions onto goethite, activated carbon and their composite: Kinetic and thermodynamic studies. *Applied Water Science* **10**(9), 1–18.

Aigbe, U. O. & Osibote, O. A. 2020 A review of hexavalent chromium removal from aqueous solutions by sorption technique using nanomaterials. *Journal of Environmental Chemical Engineering* **8** (6), 104503.

Al-Abbad, E., Alakhras, F., Anastopoulos, I., Das, D., AL-Arfaj, A., Ouerfelli, N. & Hosseini-Bandegharaei, A. 2020 Chitosan-based materials for the removal of nickel ions from aqueous solutions. *Russian Journal of Physical Chemistry A* **94**, 748–755.

Alasadi, A., Khaili, F. & Awwad, A. 2019 Adsorption of Cu (II), Ni (II) and Zn (II) ions by nano kaolinite: thermodynamics and kinetics studies. *Chemistry International* **5**(4), 258–226.

An, Y., Zhang, X., Wang, X., Chen, Z. & Wu, X. 2018 Nano@ lignocellulose intercalated montmorillonite as adsorbent for effective Mn (II) removal from aqueous solution. *Scientific Reports* **8**(1), 1–11.

An, Q., Jiang, Y.-Q., Nan, H.-Y., Yu, Y. & Jiang, J.-N. 2019 Unraveling sorption of nickel from aqueous solution by KMnO4 and KOH-modified peanut shell biochar: Implicit mechanism. *Chemosphere* **214**, 846–854.

Anand, S. R., Aggarwal, R., Saini, D., Sonker, A. K., Chauhan, N. & Sonkar, S. K. 2019 Removal of toxic chromium (VI) from the wastewater under the sunlight-illumination by functionalized carbon nano-rods. *Solar Energy* **193**, 774–781.

Arim, A. L., Guzzo, G., Quina, M. J. & Gando-Ferreira, L. M. 2018 Single and binary sorption of Cr (III) and Ni (II) onto modified pine bark. *Environmental Science and Pollution Research* **25**(28), 28039–28049.

Aslan, S., Yildiz, S. & Ozturk, M. 2018 Biosorption of Cu^{2+} and Ni^{2+} ions from aqueous solutions using waste dried activated sludge biomass. *Polish Journal of Chemical Technology* **20**(3), 20–28.

Aslani, H., Kosari, T. E., Naseri, S., Nabizadeh, R. & Khazaei, M. 2018 Hexavalent chromium removal from aqueous solution using functionalized chitosan as a novel nano-adsorbent: Modeling and optimization, kinetic, isotherm, and thermodynamic studies, and toxicity testing. *Environmental Science and Pollution Research* **25**(20), 20154–20168.

Ates, N. & Basak, A. 2019 Selective removal of aluminum, nickel and chromium ions by polymeric resins and natural zeolite from anodic plating wastewater. *International Journal of Environmental Health Research* **31** (1), 102–119.

Balasubramanian, U. M., Murugaiyan, S. V. & Marimuthu, T. 2019 Enhanced adsorption of Cr (VI), Ni (II) ions from aqueous solution using modified *Eichhornia crassipes* and *Lemna minor*. *Environmental Science and Pollution Research* **27**, 20648–20662.

Bao, S., Yang, W., Wang, Y., Yu, Y. & Sun, Y. 2020 One-pot synthesis of magnetic graphene oxide composites as an efficient and recoverable adsorbent for Cd (II) and Pb (II) removal from aqueous solution. *Journal of Hazardous Materials* **381**, 120914.

Barsbay, M., Kavaklı, P. A., Tilki, S., Kavaklı, C. & Güven, O. 2018 Porous cellulosic adsorbent for the removal of Cd (II), Pb (II) and Cu (II) ions from aqueous media. *Radiation Physics and Chemistry* **142**, 70–76.

Bhowmik, K. L., Kanmani, M., Deb, A., Debnath, A., Nath, R. K. & Saha, B. 2018 Mesoporous iron-manganese magnetic bimetal oxide for efficient removal of Cr (VI) from synthetic aqueous solution. *Applied Mechanics and Materials* **877**, 33–38.

Brodin, F. W., Gregersen, Ø. W. & Syverud, K. 2014 Cellulose nanofibrils: Challenges and possibilities as a paper additive or coating material–a review. *Nordic Pulp & Paper Research Journal* **29**(1), 156–166.

Dehghani, M. H., Niasar, Z. S., Mehrnia, M. R., Shayeghi, M., Al-Ghouti, M. A., Heibati, B., McKay, G. & Yetilmezsoy, K. 2017 Optimizing the removal of organophosphorus pesticide malathion from water using multi-walled carbon nanotubes. *Chemical Engineering Journal* **310**, 22–32.

Dehghani, M. H., Sarmadi, M., Alipour, M. R., Sanaei, D., Abdolmaleki, H., Agarwal, S. & Gupta, V. K. 2019 Investigating the equilibrium and adsorption kinetics for the removal of Ni (II) ions from aqueous solutions using adsorbents prepared from the modified waste newspapers: A low-cost and available adsorbent. *Microchemical Journal* **146**, 1043–1053.

Dim, P., Mustapha, L., Termtanun, M. & Okafor, J. 2021 Adsorption of chromium (VI) and iron (III) ions onto acid-modified kaolinite: isotherm, kinetics and thermodynamics studies. *Arabian Journal of Chemistry* **14**(4), 103064.

Esmaeili, A. & Beni, A. A. 2018 Optimization and design of a continuous biosorption process using brown algae and chitosan/PVA nano-fiber membrane for removal of nickel by a new biosorbent. *International Journal of Environmental Science and Technology* **15**(4), 765–778.

Fan, X., Xia, J. & Long, J. 2019 The potential of nonliving *Sargassum hemiphyllum* as a biosorbent for nickel (II) removal – isotherm, kinetics, and thermodynamics analysis. *Environmental Progress & Sustainable Energy* **38**(s1), S250–S259.

Farokhi, M., Parvareh, A. & Moraveji, M. K. 2018 Performance of ceria/iron oxide nano-composites based on chitosan as an effective adsorbent for removal of Cr (VI) and Co (II) ions from aqueous systems. *Environmental Science and Pollution Research* **25**(27), 27059–27073.

Ferrer, A., Quintana, E., Filpponen, I., Solala, I., Vidal, T., Rodríguez, A., Laine, J. & Rojas, O. J. 2012 Effect of residual lignin and heteropolysaccharides in nanofibrillar cellulose and nanopaper from wood fibers. *Cellulose* **19**(6), 2179–2193.

Gebru, K. A. & Das, C. 2018 Removal of chromium (VI) ions from aqueous solutions using amine-impregnated TiO_2 nanoparticles modified cellulose acetate membranes. *Chemosphere* **191**, 673–684.

Guo, X., Tang, S., Song, Y. & Nan, J. 2018 Adsorptive removal of Ni^{2+} and Cd^{2+} from wastewater using a green longan hull adsorbent. *Adsorption Science & Technology* **36**(1–2), 762–773.

Hachoumi, I., Benkaddour, S., El Ouahabi, I., Slimani, R., Cagnon, B., El Haddad, M., El Antri, S. & Lazar, S. 2019 Ensis siliqua shell for removal of Cu (II), Zn (II) and Ni (II) from aqueous solutions: Kinetics and isotherm model. *Analytical Chemistry Letters* **9**(1), 50–63.

Hadadian, M., Goharshadi, E. K., Fard, M. M. & Ahmadzadeh, H. 2018 Synergistic effect of graphene nanosheets and zinc oxide nanoparticles for effective adsorption of Ni (II) ions from aqueous solutions. *Applied Physics A* **124**(3), 239.

Hosseini, H., Rezaei, H., Shahbazi, A. & Maghsoodlu, A. 2016 Application of nano-lignocellulose for removal of nickel ions from aqueous solutions. *Environmental Resources Research* **4**(2), 213–229.

Huang, H., He, D., Tang, Y., Guo, Y., Li, P., Qv, W., Deng, F. & Lu, F. 2018 Adsorption of hexavalent chromium from an aqueous phase by hydroxypropyl methylcellulose modified with diethylenetriamine. *Journal of Chemical & Engineering Data* **64**(1), 98–106.

Ji, Y., Wen, Y., Wang, Z., Zhang, S. & Guo, M. 2020 Eco-friendly fabrication of a cost-effective cellulose nanofiber-based aerogel for multifunctional applications in Cu (II) and organic pollutants removal. *Journal of Cleaner Production* **255**, 120276.

Jiang, D., Yang, Y., Huang, C., Huang, M., Chen, J., Rao, T. & Ran, X. 2019 Removal of the heavy metal ion nickel (II) via an adsorption method using flower globular magnesium hydroxide. *Journal of Hazardous Materials* **373**, 131–140.

Kaewsichan, L. & Tohdee, K. 2019 Adsorption of hexavalent chromium onto alkali-modified biochar derived from *Lepironia articulata*: A kinetic, equilibrium, and thermodynamic study. *Water Environment Research* **91**(11), 1433–1446.

Khelifi, O., Nacef, M. & Affoune, A. M. 2018 Nickel (II) adsorption from aqueous solutions by physico-chemically modified sewage sludge. *Iranian Journal of Chemistry and Chemical Engineering (IJCCE)* **37**(1), 73–87.

Kong, A., Ji, Y., Ma, H., Song, Y., He, B. & Li, J. 2018 A novel route for the removal of Cu (II) and Ni (II) ions via homogeneous adsorption by chitosan solution. *Journal of Cleaner Production* **192**, 801–808.

Kumar, R. & Sharma, R. K. 2019 Synthesis and characterization of cellulose based adsorbents for removal of Ni (II), Cu (II) and Pb (II) ions from aqueous solutions. *Reactive and Functional Polymers* **140**, 82–92.

Kumar, R., Kim, S.-J., Kim, K.-H., Lee, S.-h., Park, H.-S. & Jeon, B.-H. 2018 Removal of hazardous hexavalent chromium from aqueous phase using zirconium oxide-immobilized alginate beads. *Applied Geochemistry* **88**, 113–121.

Kumar, R., Sharma, R. K. & Singh, A. P. 2019a Grafting of cellulose with N-isopropylacrylamide and glycidyl methacrylate for efficient removal of Ni (II), Cu (II) and Pd (II) ions from aqueous solution. *Separation and Purification Technology* **219**, 249–259.

Kumar, R., Sharma, R. K. & Singh, A. P. 2019b Sorption of Ni (II), Pb (II) and Cu (II) ions from aqueous solutions by cellulose grafted with poly (HEMA-co-AAc): Kinetic isotherm and thermodynamic study. *Journal of Environmental Chemical Engineering* **7**(3), 103088.

Kundu, D., Mondal, S. K. & Banerjee, T. 2019 Development of β-cyclodextrin-cellulose/hemicellulose-based hydrogels for the removal of Cd (II) and Ni (II): Synthesis, kinetics, and adsorption aspects. *Journal of Chemical & Engineering Data* **64**(6), 2601–2617.

Langmuir, I. 1918 The adsorption of gases on plane surfaces of glass, mica and platinum. *Journal of the American Chemical Society* **40**(9), 1361–1403.

Mahmoud, M. E., Amira, M. F., Seleim, S. M. & Mohamed, A. K. 2020 Amino-decorated magnetic metal-organic framework as a potential novel platform for selective removal of chromium (Vl), cadmium (II) and lead (II). *Journal of Hazardous Materials* **381**, 120979.

Maleki, A., Hajizadeh, Z., Sharifi, V. & Emdadi, Z. 2019 A green, porous and eco-friendly magnetic geopolymer adsorbent for heavy metals removal from aqueous solutions. *Journal of Cleaner Production* **215**, 1233–1245.

Manjuladevi, M., Anitha, R. & Manonmani, S. 2018 Kinetic study on adsorption of Cr (VI), Ni (II), Cd (II) and Pb (II) ions from aqueous solutions using activated carbon prepared from Cucumis melo peel. *Applied Water Science* **8**(1), 36.

Mondal, N. K. & Chakraborty, S. 2020 Adsorption of Cr (VI) from aqueous solution on graphene oxide (GO) prepared from graphite: equilibrium, kinetic and thermodynamic studies. *Applied Water Science* **10**(2), 1–10.

Mousavi, S. V., Bozorgian, A., Mokhtari, N., Gabris, M. A., Nodeh, H. R. & Ibrahim, W. A. W. 2019 A novel cyanopropylsilane-functionalized titanium oxide magnetic nanoparticle for the adsorption of nickel and lead ions from industrial wastewater: Equilibrium, kinetic and thermodynamic studies. *Microchemical Journal* **145**, 914–920.

Panagopoulos, A. 2022a Brine management (saline water & wastewater effluents): sustainable utilization and resource recovery strategy through Minimal and Zero Liquid Discharge (MLD & ZLD) desalination systems. *Chemical Engineering and Processing-Process Intensification* **176**, 108944.

Panagopoulos, A. 2022b Process simulation and analysis of high-pressure reverse osmosis (HPRO) in the treatment and utilization of desalination brine (saline wastewater). *International Journal of Energy Research* **46** (15), 23083–23094.

Panagopoulos, A. & Giannika, V. 2022 Decarbonized and circular brine management/valorization for water and valuable resource recovery via minimal/zero liquid discharge (MLD/ZLD) strategies. *Journal of Environmental Management* **324**, 116239.

Peng, H., Leng, Y. & Guo, J. 2019 Electrochemical removal of chromium (VI) from wastewater. *Applied Sciences* **9**(6), 1156.

Peter, Z. 2020 Order in cellulosics: historical review of crystal structure research on cellulose. *Carbohydrate Polymers* **254**, 117417.

Qu, J., Tian, X., Jiang, Z., Cao, B., Akindolie, M. S., Hu, Q., Feng, C., Feng, Y., Meng, X. & Zhang, Y. 2020 Multi-component adsorption of Pb (II), Cd (II) and Ni (II) onto microwave-functionalized cellulose: Kinetics, isotherms, thermodynamics, mechanisms and application for electroplating wastewater purification. *Journal of Hazardous Materials* **387**, 121718.

Qureshi, M. I., Patel, F., Al-Baghli, N., Abussaud, B., Tawabini, B. S. & Laoui, T. 2017 A comparative study of raw and metal oxide impregnated carbon nanotubes for the adsorption of hexavalent chromium from aqueous solution. *Bioinorganic Chemistry and Applications* **2017**, 1624243.

Rizzo, C., Andrews, J. L., Steed, J. W. & D'Anna, F. 2019 Carbohydrate-supramolecular gels: adsorbents for chromium (VI) removal from wastewater. *Journal of Colloid and Interface Science* **548**, 184–196.

Rodiguez, M. H., Yperman, J., Carleer, R., Maggen, J., Dadi, D., Gryglewicz, G., Van der Bruggen, B., Hernández, J. F. & Calvis, A. O. 2018 Adsorption of Ni (II) on spent coffee and coffee husk based activated carbon. *Journal of Environmental Chemical Engineering* **6**(1), 1161–1170.

Sarici-Ozdemir, C. 2012 Adsorption and desorption kinetics behaviour of methylene blue onto activated carbon. *Physicochemical Problems of Mineral Processing* **48**(2), 441–454.

Sethy, T. R. & Sahoo, P. K. 2019 Highly toxic Cr (VI) adsorption by (chitosan-g-PMMA)/silica bionanocomposite prepared via emulsifier-free emulsion polymerisation. *International Journal of Biological Macromolecules* **122**, 1184–1190.

Shao, Z., Huang, C., Wu, Q., Zhao, Y., Xu, W., Liu, Y., Dang, J. & Hou, H. 2019 Ion exchange collaborating coordination substitution: More efficient Cr (VI) removal performance of a water-stable CuII-MOF material. *Journal of Hazardous Materials* **378**, 120719.

Sheikhi, M. & Rezaei, H. 2021 Adsorption of hexavalent chromium ions from aqueous solutions using nano-chitin: Kinetic, isotherms and thermodynamic studies. *Water Practice & Technology* **16**(2), 436–451.

Shi, Y., Zhang, T., Ren, H., Kruse, A. & Cui, R. 2018 Polyethylene imine modified hydrochar adsorption for chromium (VI) and nickel (II) removal from aqueous solution. *Bioresource Technology* **247**, 370–379.

Siddiqui, M. N., Ali, I., Asim, M. & Chanbasha, B. 2020 Quick removal of nickel metal ions in water using asphalt-based porous carbon. *Journal of Molecular Liquids* **308**, 113078.

Siuki, A. K., Shahidi, A., Taherian, P. & Zeraatkar, Z. 2021 Comparing natural and mineral adsorbents in removing chromium from aquatic environment. *Ain Shams Engineering Journal* **12**(3), 2593–2601.

Sivakumar, D., Nouri, J., Modhini, T. & Deepalakshmi, K. 2018 Nickel removal from electroplating industry wastewater: A bamboo activated carbon. *Global Journal of Environmental Science and Management* **4**(3), 325–338.

Sohail, I., Bhatti, I. A., Ashar, A., Sarim, F. M., Mohsin, M., Naveed, R., Yasir, M., Iqbal, M. & Nazir, A. 2020 Polyamidoamine (PAMAM) dendrimers synthesis, characterization and adsorptive removal of nickel ions from aqueous solution. *Journal of Materials Research and Technology* **9**(1), 498–506.

Sun, L., Wang, J., Wu, J., Wang, T., Du, Y., Li, Y. & Li, H. 2019 Constructing nanostructured silicates on diatomite for Pb (II) and Cd (II) removal. *Journal of Materials Science* **54**(9), 6882–6894.

Veloso, C., Filippov, L., Filippova, I., Ouvrard, S. & Araujo, A. 2020 Adsorption of polymers onto iron oxides: Equilibrium isotherms. *Journal of Materials Research and Technology* **9**(1), 779–788.

Vilela, P. B., Dalalibera, A., Duminelli, E. C., Becegato, V. A. & Paulino, A. T. 2019 Adsorption and removal of chromium (VI) contained in aqueous solutions using a chitosan-based hydrogel. *Environmental Science and Pollution Research* **26**(28), 28481–28489.

Wu, Y., Cha, L., Fan, Y., Fang, P., Ming, Z. & Sha, H. 2017 Activated biochar prepared by pomelo peel using H 3 PO 4 for the adsorption of hexavalent chromium: performance and mechanism. *Water, Air, & Soil Pollution* **228**(10), 1–13.

Xavier, A. L. P., Adarme, O. F. H., Furtado, L. M., Ferreira, G. M. D., da Silva, L. H. M., Gil, L. F. & Gurgel, L. V. A. 2018 Modeling adsorption of copper (II), cobalt (II) and nickel (II) metal ions from aqueous solution onto a new carboxylated sugarcane bagasse. Part II: Optimization of monocomponent fixed-bed column adsorption. *Journal of Colloid and Interface Science* **516**, 431–445.

Yousefhashemi, S. M., Khosravani, A. & Yousefi, H. 2019 Isolation of lignocellulose nanofiber from recycled old corrugated container and its interaction with cationic starch–nanosilica combination to make paperboard. *Cellulose* **26**(12), 7207–7221.

Yu, J., Zhang, J., Song, S., Liu, H., Guo, Z. & Zhang, C. 2019 Removal of Ni (II) from aqueous solutions using activated carbon with manganese formate hydrate in-situ modification. *Colloids and Surfaces A: Physicochemical and Engineering Aspects* **560**, 84–91.

Zhang, L., Lu, H., Yu, J., Fan, Y., Yang, Y., Ma, J. & Wang, Z. 2018 Synthesis of lignocellulose-based composite hydrogel as a novel biosorbent for Cu^{2+} removal. *Cellulose* **25**(12), 7315–7328.

Zhang, B., Wu, Y. & Fan, Y. 2019 Synthesis of novel magnetic NiFe 2 O 4 nanocomposite grafted chitosan and the adsorption mechanism of Cr (VI). *Journal of Inorganic and Organometallic Polymers and Materials* **29**(1), 290–301.

Zhang, J., Xue, C.-H., Ma, H.-R., Ding, Y.-R. & Jia, S.-T. 2020 Fabrication of PAN electrospun nanofibers modified by tannin for effective removal of trace Cr (III) in organic complex from wastewater. *Polymers* **12**(1), 210.

Zhou, Z., Kong, D., Zhu, H., Wang, N., Wang, Z., Wang, Q., Liu, W., Li, Q., Zhang, W. & Ren, Z. 2018 Preparation and adsorption characteristics of an ion-imprinted polymer for fast removal of Ni (II) ions from aqueous solution. *Journal of Hazardous Materials* **341**, 355–364.

First received 2 September 2022; accepted in revised form 31 March 2023. Available online 11 April 2023